AMERICAN SOCIETY FOR MICROBIOLOGY | Infection and Immunity®

BACTERIAL INFECTIONS

NLRP3 Is a Critical Regulator of Inflammation and Innate Immune Cell Response during *Mycoplasma pneumoniae* Infection

Jesus A. Segovia,[a] Te-Hung Chang,[a] Vicki T. Winter,[b] Jacqueline J. Coalson,[b] Marianna P. Cagle,[a] Lavanya Pandranki,[a] Santanu Bose,[c] Joel B. Baseman,[a] Thirumalai R. Kannan[a]

[a]Department of Microbiology, Immunology and Molecular Genetics, University of Texas Health Science Center at San Antonio, San Antonio, Texas, USA

[b]Department of Pathology, University of Texas Health Science Center at San Antonio, San Antonio, Texas, USA

[c]Department of Veterinary Microbiology and Pathology, Washington State University, Pullman, Washington, USA

ABSTRACT *Mycoplasma pneumoniae* is an atypical bacterial respiratory pathogen known to cause a range of airway inflammation and lung and extrapulmonary pathologies. We recently reported that an *M. pneumoniae*-derived ADP-ribosylating and vacuolating toxin called community-acquired respiratory distress syndrome (CARDS) toxin is capable of triggering NLRP3 (NLR-family, leucine-rich repeat protein 3) inflammasome activation and interleukin-1β (IL-1β) secretion in macrophages. However, it is unclear whether the NLRP3 inflammasome is important for the immune response during *M. pneumoniae* acute infection. In the current study, we utilized *in vitro* and *in vivo* models of *M. pneumoniae* infection to characterize the role of the NLRP3 inflammasome during acute infection. *M. pneumoniae*-infected macrophages deficient for inflammasome components NLRP3, ASC (apoptosis speck-like protein containing a caspase activation and recruitment domain), or caspase-1 failed to process and secrete IL-1β. The MyD88/NF-κB signaling pathway was found to be critical for proinflammatory gene expression in macrophages infected with *M. pneumoniae*. C57BL/6 mice deficient for NLRP3 expression were unable to produce IL-1β in the airways during acute infection, and lack of this inflammatory response led to deficient immune cell activation and delayed bacterial clearance. These findings are the first to report the importance of the NLRP3 inflammasome in regulating the inflammatory response and influencing the progression of *M. pneumoniae* during acute infection.

KEYWORDS ADP-ribosylation, CARDS toxin, *Mycoplasma pneumoniae*, NLRP3, inflammasome, interleukin-1β

Mycoplasma pneumoniae is an atypical bacterium that causes acute and chronic respiratory tract infections in humans. *M. pneumoniae* is a significant cause of community-acquired pneumonia and has been implicated in the initiation and exacerbation of asthma (1–4). Furthermore, *M. pneumoniae* outbreaks are an important public health concern since numerous strains exhibiting antibiotic resistance are emerging worldwide (5, 6). Cytadherence to the mucosal epithelium via the major adhesin protein P1 constitutes a key virulence factor of *M. pneumoniae* (7). Hydrogen peroxide and superoxide radicals generated following mycoplasma cytadherence are considered additional virulence factors (8). The degree to which *M. pneumoniae* causes severe disease can be attributed in part to the expression of these virulence factors and the host immune response during infection (4, 8–10).

We reported previously that *M. pneumoniae* produces a protein toxin of 591 amino acids, designated the community-acquired respiratory distress syndrome (CARDS) toxin

Received 1 August 2017 **Returned for modification** 24 August 2017 **Accepted** 16 October 2017

Accepted manuscript posted online 23 October 2017

Citation Segovia JA, Chang T-H, Winter VT, Coalson JJ, Cagle MP, Pandranki L, Bose S, Baseman JB, Kannan TR. 2018. NLRP3 is a critical regulator of inflammation and innate immune cell response during *Mycoplasma pneumoniae* infection. Infect Immun 86:e00548-17. https://doi.org/10.1128/IAI.00548-17.

Editor Sabine Ehrt, Weill Cornell Medical College

Address correspondence to Thirumalai R. Kannan, kannan@uthscsa.edu.

(11, 12). CARDS toxin contains both ADP-ribosyltransferase and vacuolating activities located in separate domains, a combination that is distinct among all bacterial toxins (13, 14). Interestingly, CARDS toxin alone can elicit many of the hallmark pathological features evident during and after *M. pneumoniae* infection, including loss of respiratory epithelium integrity, ciliostasis, cellular vacuolization and swelling, histopathology, and mucus metaplasia (12, 15). Importantly, CARDS toxin expression is highly upregulated during infection, and its presence can be readily detected in airway samples from *M. pneumoniae*-infected mice and humans (16, 17). Our recent studies uncovered an intriguing mechanism by which CARDS toxin triggers secretion of interleukin-1β (IL-1β) via direct ADP-ribosylation of NLRP3 (NLR-family, leucine-rich repeat protein 3), the major component of the NLRP3 inflammasome complex (18).

During infection, pathogenic determinants trigger NLRP3 to self-oligomerize and recruit ASC (apoptosis-associated speck-like protein containing a caspase activation and recruitment domain) and procaspase-1. Tight aggregation of procaspase-1 triggers autocleavage into p10 and p20 subunits, which heterodimerize to form active caspase-1 enzyme, resulting in the rapid processing of pro-IL-1β into biologically active IL-1β p17 (19). IL-1β secreted into the extracellular environment can amplify the inflammatory response via paracrine or autocrine mechanisms. Inflammasome activation is preceded by signaling events that are triggered in response to detection of pathogens or pathogenic stimuli (20). Following stimulation, Toll-like receptors (TLRs) trigger activation of the MyD88/NF-κB or TRIF/NF-κB pathway, leading to enhanced expression of proinflammatory genes, such as pro-IL-1β (21).

Macrophages are important producers of IL-1β and are among the predominant immune cells that first interact with *M. pneumoniae* during infection (22). *M. pneumoniae* infection triggers secretion of several proinflammatory cytokines, including tumor necrosis factor alpha (TNF-α), IL-6, and, importantly, IL-1β (23). Although CARDS toxin was previously found to utilize an NLRP3-dependent mechanism to induce IL-1β release from macrophages *in vitro*, the mechanism by which *M. pneumoniae* triggers IL-1β secretion during infection is presently unclear. Furthermore, it is also unknown whether *M. pneumoniae* infection initiates IL-1β secretion primarily through NLRP3 inflammasome activation and whether it plays an important role in shaping the immune response during infection in the respiratory tract. In our current study, we established a critical function for the NLRP3 inflammasome during *in vitro* and *in vivo* *M. pneumoniae* infection. *M. pneumoniae* infection triggers caspase-1 activation and IL-1β secretion using an NLRP3/ASC inflammasome-dependent mechanism in mouse bone marrow-derived macrophages (BMDMs). MyD88-dependent NF-κB signaling was required for a maximal inflammatory response during infection. Importantly, infected NLRP3 knockout (KO) C57BL/6 mice displayed diminished IL-1β cytokine secretion and bacterial clearance and incomplete innate immune cell activation compared to results in infected wild-type (WT) C57BL/6 mice. Our findings demonstrate that *M. pneumoniae* infection activates the NLRP3 inflammasome complex, leading to IL-1β secretion, inflammation, and innate immune cell activation in the lungs of infected C57BL/6 mice. These results also indicate that NLRP3 is critical for recruitment and activation of neutrophils, dendritic cells (DCs), and inflammatory macrophages (IMs) during *M. pneumoniae* acute infection.

RESULTS

***M. pneumoniae* infection induces a strong proinflammatory cytokine response in primary mouse macrophages.** *M. pneumoniae* is known to elicit the production of numerous proinflammatory cytokines and chemokines during acute infection. Furthermore, because CARDS toxin alone provokes a selective inflammasome-based cytokine response, we sought to broadly characterize the immune response to *M. pneumoniae* organisms in primary mouse BMDMs. Cell culture supernatants of WT BMDMs infected with *M. pneumoniae* were analyzed for cytokine levels using a multiplex bead array (Fig. 1). The proinflammatory cytokines IL-1α, IL-1β, IL-6, and TNF-α were secreted following *M. pneumoniae* infection as early as 4 h postinfection; IL-6 and TNF-α levels rose sharply

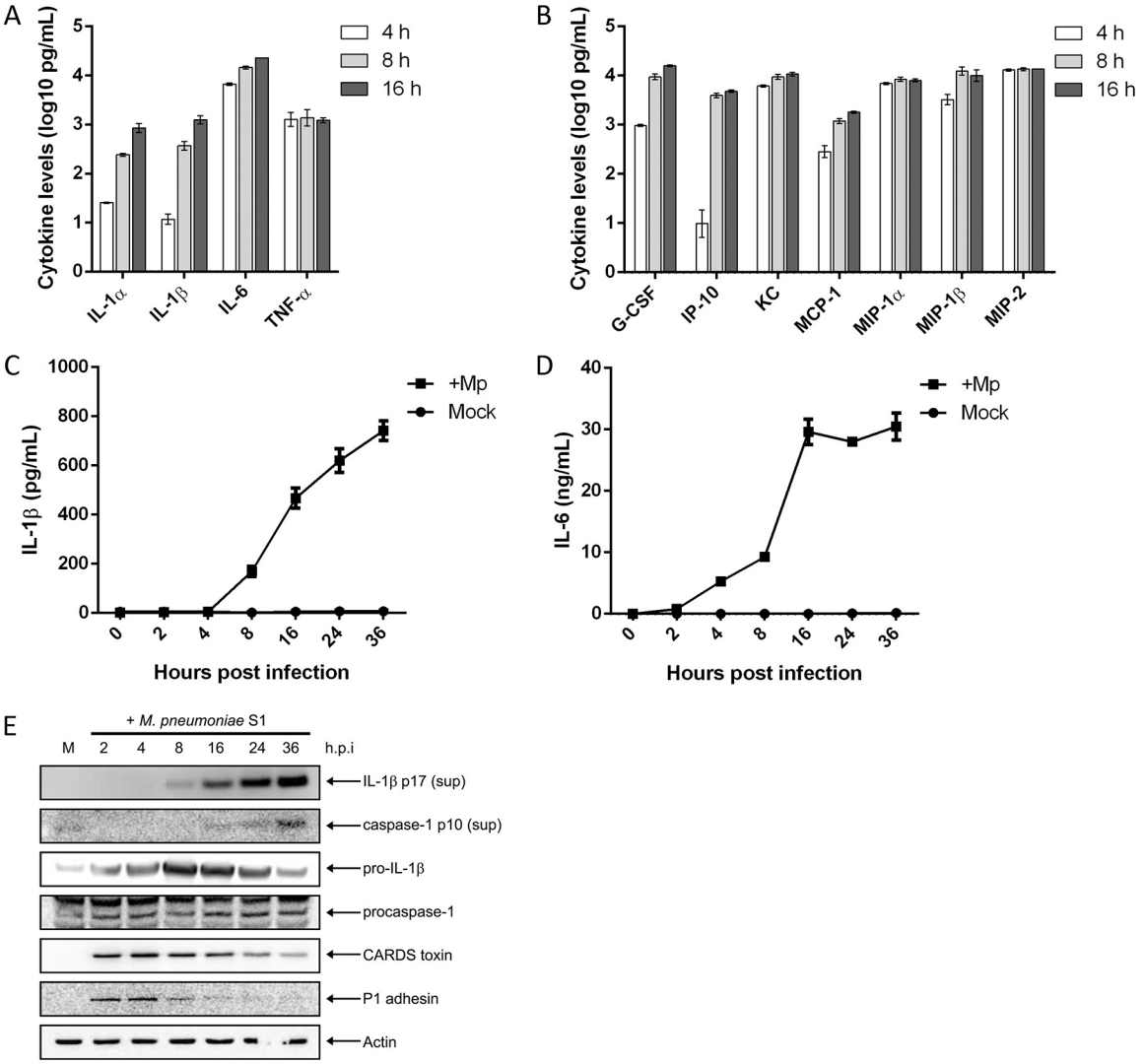

FIG 1 Primary macrophages infected with *M. pneumoniae* produce proinflammatory and chemotactic cytokines. WT BMDMs were infected with *M. pneumoniae* at an MOI of 100 mycoplasmas per cell. At 4, 8, and 16 h postinfection, cell culture supernatants were collected and used in multiplex cytokine bead assays. Values for proinflammatory cytokines (A) and other cytokines and chemokines (B) were normalized by subtracting values of the uninfected control from those of the infected animals and are represented in log scale. Time course kinetics for IL-1β and IL-6 secretion are shown in panels C and D, respectively. (E) Immunoblot analysis of IL-1β p17 and caspase-1 p10 in cell culture supernatants (sup) and pro-IL-1β, procaspase-1, CARDS toxin, and P1 adhesin in cell lysates of WT BMDMs infected with *M. pneumoniae*. The mock-infected control is designated M. β-Actin served as the loading control. Data in panels A and B are representative of two independent experiments with similar results; data in panels C and D are representative of two independent experiments with similar results. h.p.i., hours postinfection; Mp, *M. pneumoniae*. All cytokine and chemokine levels are listed in Table S1 in the supplemental material.

and remained at high levels whereas IL-1α and IL-1β levels rose steadily through the course of infection (Fig. 1A). The cytokines and chemokines granulocyte colony-stimulating factor (G-CSF), IP-10, keratinocyte-derived chemokine (KC), monocyte chemoattractant protein 1 (MCP-1), macrophage inflammatory protein 1α (MIP-1α), MIP-1β, and MIP-2 were also secreted following *M. pneumoniae* infection of BMDMs (Fig. 1B). Raw cytokine and chemokine values for mock- and *M. pneumoniae*-infected samples in Fig. 1 are listed in Table S1 in the supplemental material. This cytokine and chemokine profile accurately reflects reports of *M. pneumoniae* infection in both mice and humans (15, 24).

We next sought to characterize the temporal processing of IL-1β during *M. pneumoniae* infection. Infection of WT BMDMs leads to rapid secretion of the proinflammatory cytokines IL-6 and IL-1β into the cell culture supernatant. IL-1β is detectable in

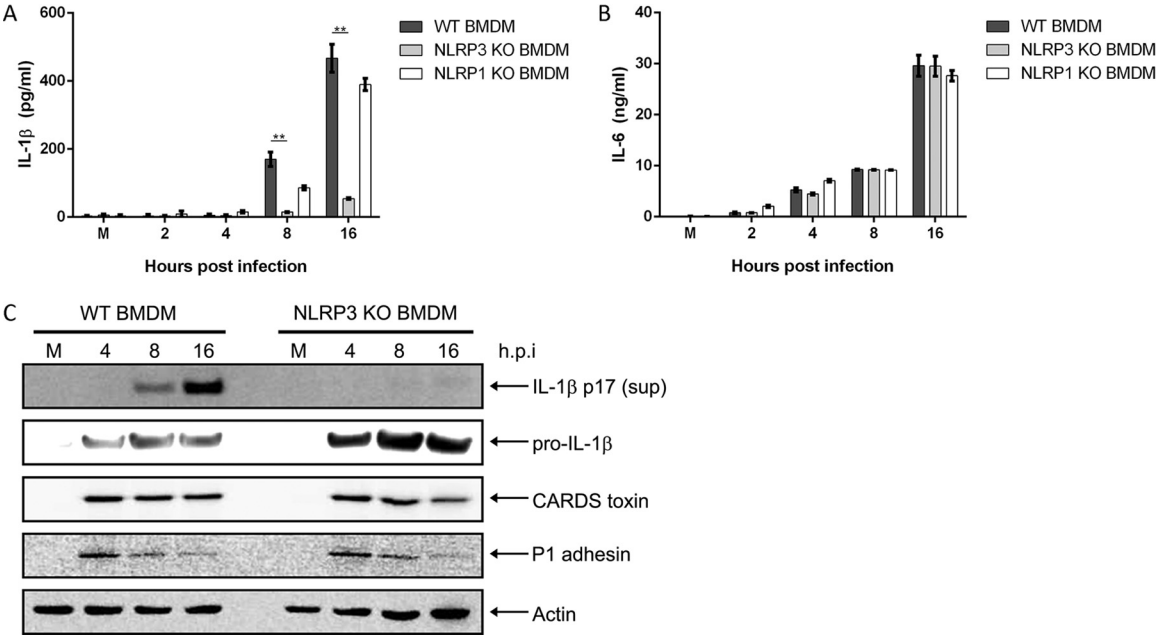

FIG 2 NLRP3, but not NLRP1, is required for inflammasome activation and IL-1β secretion during *M. pneumoniae* infection. Cell culture supernatants from WT, NLRP3 KO, and NLRP1 KO BMDMs infected with *M. pneumoniae* were assayed by ELISA for IL-1β (A) and IL-6 (B) levels. (C) Immunoblot analysis of IL-1β p17 in supernatants and pro-IL-1β, CARDS toxin, and P1 adhesin in cell lysates of WT and NLRP3 KO BMDMs infected with *M. pneumoniae*. The mock-infected control is designated M. β-Actin served as the loading control. Data are representative of three independent experiments with similar results. **, $P < 0.01$. h.p.i., hours postinfection.

culture supernatants as early as 4 h postinfection in very small quantities (~10 to 15 pg/ml), and secretion increases gradually as the infection persists (Fig. 1C) while IL-6 is detected as early as 2 h postinfection in the supernatants (Fig. 1D). IL-1β p17 is detectable at 8 h postinfection in the supernatants of infected cells by immunoblot analysis (Fig. 1E). In mock-infected controls, IL-1β and IL-6 were undetectable at all time points (Fig. 1C and D). Interestingly, analysis of cell lysates revealed that pro-IL-1β is expressed as early as 2 h postinfection (Fig. 1E). Processing of the precursor protein pro-IL-1β to biologically active mature IL-1β requires activated caspase-1. As the time course demonstrates (Fig. 1E), *M. pneumoniae* infection triggered activation of procaspase-1, resulting in release of the caspase-1 p10 subunit into cell culture supernatants at 16 h postinfection, around the same time when mature IL-1β can be readily detected. Early detection of *M. pneumoniae* P1 adhesin protein in the macrophage cell lysate indicates mycoplasma infection although P1 protein levels drop off dramatically beginning at 8 h postinfection (Fig. 1E). Interestingly, CARDS toxin protein levels in the cell lysate peak at 4 h postinfection and remain readily detectable throughout the duration of the infection (Fig. 1E).

NLRP3 is required for inflammasome activation and IL-1β processing during *M. pneumoniae* infection. The temporal relationship between CARDS toxin and IL-1β secretion (18) prompted us to explore the role of NLRP3 during *M. pneumoniae* infection by comparing BMDMs from WT and NLRP3 KO C57BL/6 mice. Analysis of cell culture supernatants by enzyme-linked immunosorbent assay (ELISA) revealed that following *M. pneumoniae* infection, NLRP3 KO BMDMs secreted drastically reduced levels of the cytokine IL-1β compared to those of WT BMDMs (Fig. 2A). As a comparison, we also infected BMDMs from NLRP1 KO C57BL/6 mice. NLRP1 KO BMDMs infected with *M. pneumoniae* showed slightly decreased but statistically insignificant differences in IL-1β levels compared to those of WT BMDMs (Fig. 2A). Despite the differences in IL-1β secretion levels, no differences in IL-6 secretion levels were detected between WT, NLRP3 KO, and NLRP1 KO BMDMs infected with *M. pneumoniae* (Fig. 2B). Immunoblot analysis revealed pro-IL-1β protein expression in both WT and NLRP3 KO BMDMs (Fig. 2C). However, IL-1β p17 protein was detected only in the supernatants of infected WT

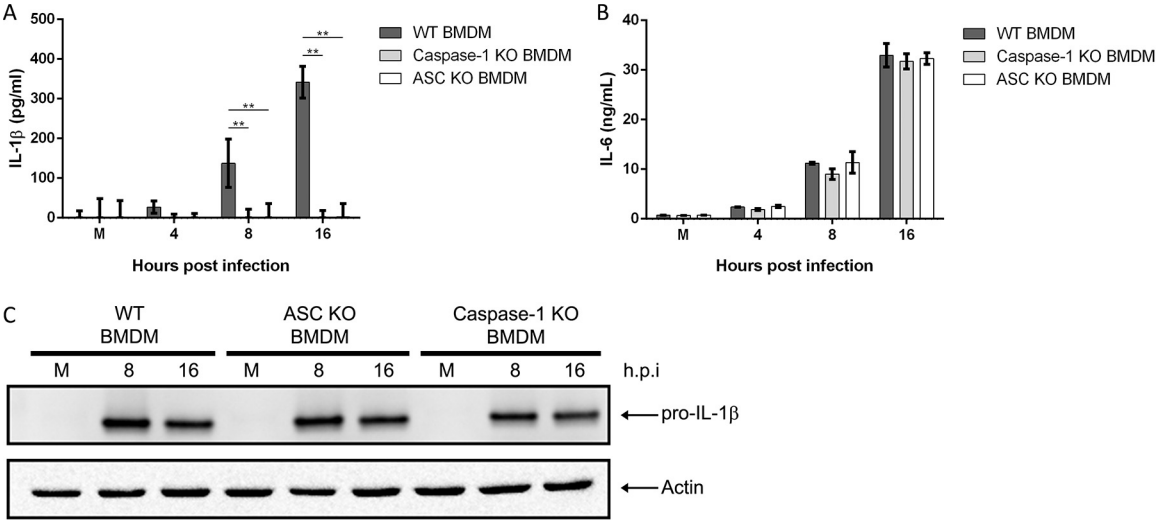

FIG 3 Caspase-1 and ASC are required for inflammasome activation and IL-1β processing during *M. pneumoniae* infection. Cell culture supernatants from WT, caspase-1 KO, and ASC KO BMDMs infected with *M. pneumoniae* were assayed by ELISA for IL-1β (A) and IL-6 (B) levels. (C) Immunoblot analysis for pro-IL-1β in cell lysates of WT, ASC KO, and caspase-1 KO BMDMs infected with *M. pneumoniae*. The mock-infected control is designated M. β-Actin served as the loading control. Data are representative of two independent experiments with similar results. **, $P < 0.01$. h.p.i., hours postinfection.

BMDMs and not in those of NLRP3 KO BMDMs (Fig. 2C). Analysis of P1 and CARDS toxin proteins in the experiment shown in Fig. 2C showed a pattern similar to that observed in the experiment shown in Fig. 1E. This pattern also held true through all remaining experiments and further implicate NLRP3 as a major inflammasome component required to trigger IL-1β processing and secretion during *M. pneumoniae* infection.

Caspase-1 and ASC are required for IL-1β processing during *M. pneumoniae* infection. Activation and oligomerization of NLRP3 lead to recruitment of ASC and procaspase-1 and formation of the inflammasome complex. We next tested the requirement of caspase-1 and ASC for inflammasome formation and IL-1β secretion. We infected WT, caspase-1 KO, and ASC KO BMDMs with *M. pneumoniae* and looked for evidence of caspase-1 activation as well as cleavage of pro-IL-1β. Analysis of cell culture supernatants by ELISA revealed complete loss of IL-1β secretion in infected caspase-1 KO and ASC KO BMDMs in contrast to results in WT BMDMs (Fig. 3A). In contrast, IL-6 secretion, which occurs independently of inflammasome activation, was at comparable levels regardless of cell type (Fig. 3B), demonstrating that the ability of *M. pneumoniae* to activate other inflammatory pathways was not compromised. Consistent with our NLRP3 data, we observed upregulation of pro-IL-1β in cell lysates of infected caspase-1 and ASC KO BMDMs (Fig. 3C). Lysates were also probed for procaspase-1 and ASC to confirm KO status (data not shown). Together, these data demonstrate that *M. pneumoniae* infection leads to caspase-1 cleavage and IL-1β processing in macrophages via the NLRP3/ASC inflammasome complex.

Proinflammatory gene upregulation during *M. pneumoniae* infection is mediated by the MyD88/NF-κB pathway. Activation of the transcription factor NF-κB is known to upregulate the expression of many proinflammatory genes, such as pro-IL-1β (25). Therefore, we tested whether the *M. pneumoniae*-induced proinflammatory response required NF-κB activation by utilizing the irreversible NF-κB inhibitor BAY11-7082. WT BMDMs were pretreated with either dimethyl sulfoxide (DMSO; vehicle control) or BAY11-7082, followed by infection with *M. pneumoniae*. Analysis of cell culture supernatants by ELISA revealed almost complete abolishment of IL-1β secretion in the BAY11-7082-treated infected cells (Fig. 4A). Since IL-6 is an NF-κB-dependent gene, IL-6 secretion was also dramatically inhibited in BAY11-7082-treated BMDMs infected with *M. pneumoniae*, as expected (Fig. 4B). Immunoblot analysis revealed complete lack of pro-IL-1β expression in lysates of BAY11-7082-treated *M. pneumoniae*-

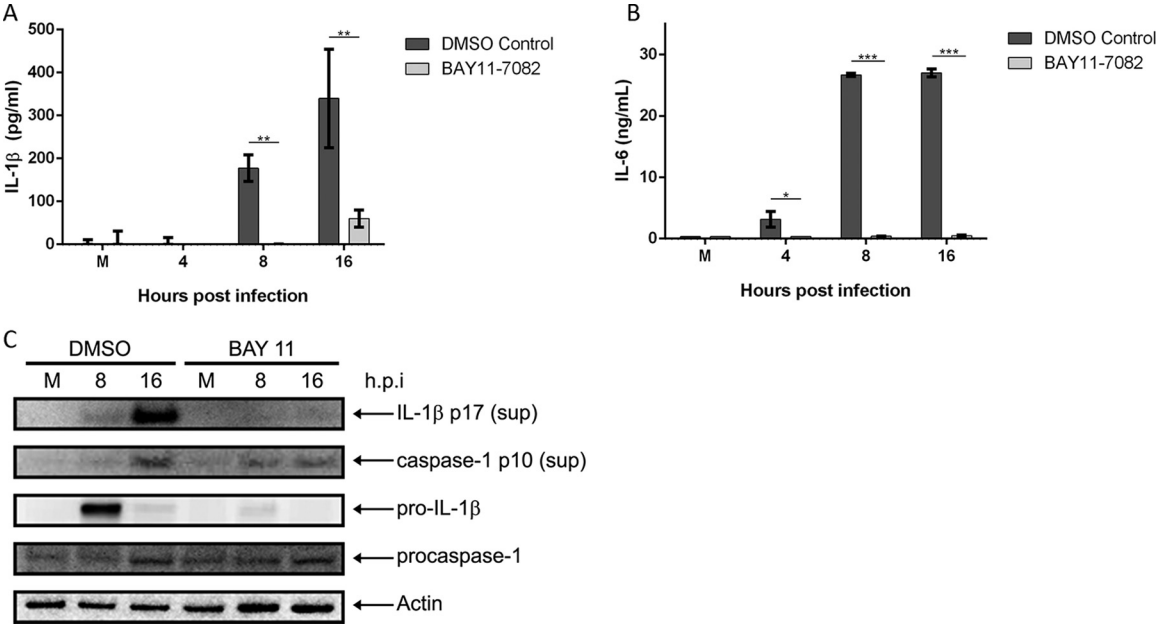

FIG 4 NF-κB signaling is required for expression of proinflammatory genes and inflammasome activation during *M. pneumoniae* infection. Cell culture supernatants from *M. pneumoniae*-infected WT BMDMs treated with the NF-κB inhibitor BAY11-7082 were assayed by ELISA for IL-1β (A) and IL-6 (B) levels. (C) Immunoblot analysis of IL-1β p17 and caspase-1 p10 in supernatants and pro-IL-1β and procaspase-1 in cell lysates of vehicle (DMSO-treated) or BAY11-7082-treated WT BMDMs infected with *M. pneumoniae*. The mock-infected control is designated M. β-Actin served as the loading control. Data are representative of three independent experiments with similar results. *, $P < 0.05$; **, $P < 0.01$; ***, $P < 0.001$. h.p.i., hours postinfection.

infected cells in contrast to results in DMSO-treated *M. pneumoniae*-infected cells (Fig. 4C). Caspase-1 p10 protein was detected in BAY11-7082-treated cells infected with *M. pneumoniae*, albeit at visibly lower levels than in DMSO-treated infected cells. This is likely due to reduced NLRP3 inflammasome activation resulting from diminished NLRP3 expression, which is regulated by NF-κB.

Next, we sought to determine if NF-κB signaling was MyD88 dependent since MyD88 represents one of the major TLR adaptor proteins required for upregulation of proinflammatory genes during infection (21). MyD88 KO BMDMs infected with *M. pneumoniae* showed complete loss of IL-1β (Fig. 5A) and IL-6 (Fig. 5B) secretion into the cell culture supernatant. Expression of pro-IL-1β protein in the cell lysates was abolished in infected MyD88 KO BMDMs (Fig. 5C). While procaspase-1 protein levels were similar between WT and MyD88 KO BMDMs, caspase-1 p10 levels were noticeably lower in the lysates of infected MyD88 KO BMDMs (similar to the results shown in Fig. 4C), indicating reduced procaspase-1 processing as a likely result of diminished NLRP3 expression. Our observations implicate the MyD88/NF-κB pathway as the critical signaling pathway necessary for detecting *M. pneumoniae* infection *in vitro*.

NLRP3 is critical for the innate immune response against *M. pneumoniae* infection *in vivo*. Our studies identified NLRP3 as indispensable for inflammasome activation and IL-1β secretion during *M. pneumoniae* infection in mouse BMDMs. Next, we determined the role of NLRP3 during *in vivo M. pneumoniae* infection. WT and NLRP3 KO C57BL/6 mice were infected intranasally with *M. pneumoniae* (7 $\log_{10}$ CFU) for 2 and 7 days, and bronchoalveolar lavage fluids (BALFs) were analyzed by ELISA to quantify levels of IL-1β and IL-6. Infected NLRP3 KO mice showed almost complete loss of IL-1β secretion into the extracellular alveolar space compared to levels in WT mice at 2 days postinfection (Fig. 6A). However, IL-6 cytokine levels were similar (Fig. 6B). IL-1β levels were undetectable in all mock-infected mice and in *M. pneumoniae*-infected mice at 7 days postinfection (data not shown). Analysis of BALFs by quantitative PCR (qPCR) revealed a significantly higher bacterial load in NLRP3 KO mice than in WT mice (2.24×10^6 versus 4.8×10^5 CFU, respectively) at 2 days postinfection (Fig. 6C). A larger

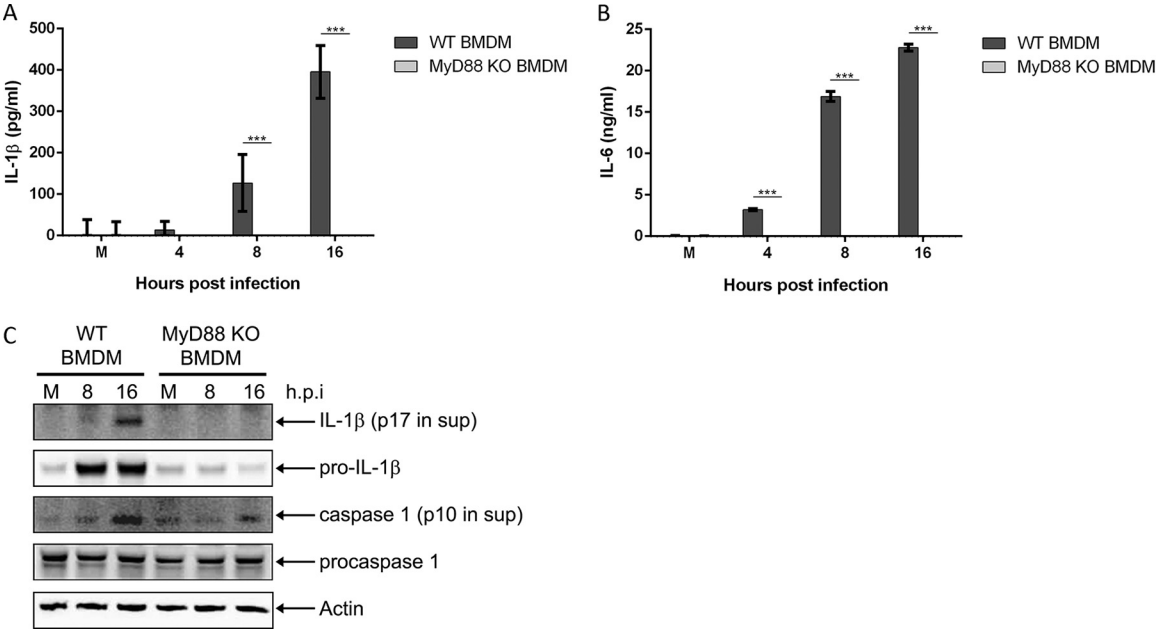

FIG 5 MyD88 signaling is required for expression of proinflammatory genes and inflammasome activation during *M. pneumoniae* infection. Cell culture supernatants from WT and MyD88 KO BMDMs infected with *M. pneumoniae* were assayed by ELISA for IL-1β (A) and IL-6 (B) levels. (C) Immunoblot analysis of IL-1β p17 and caspase-1 p10 in supernatants and pro-IL-1β and procaspase-1 in cell lysates of WT and MyD88 KO BMDMs infected with *M. pneumoniae*. The mock-infected control is designated M. β-Actin served as the loading control. Data are representative of three independent experiments with similar results. ***, $P < 0.001$. h.p.i., hours postinfection.

difference in bacterial load was present in NLRP3 KO mice than in WT mice (9.7×10^5 versus 9.8×10^4, respectively) at 7 days postinfection (Fig. 6D). These data suggest that NLRP3 is required for IL-1β secretion in the lungs during *M. pneumoniae* infection and that loss of IL-1β secretion results in reduced bacterial clearance.

Lastly, we used flow cytometry analysis in order to characterize the innate immune cell populations present in the lungs of NLRP3 KO and WT mice at 2 days postinfection. Analysis of innate immune cells revealed a significant increase in total lung CD11b$^+$ neutrophil populations following *M. pneumoniae* infection in both WT and NLRP3 KO mice compared to levels in mock-infected mice (Fig. 7A). Interestingly, the population of activated (CD11b$^+$ Ly6G$^+$) neutrophils was significantly higher in infected WT mice than in infected NLRP3 KO mice (Fig. 7B). Additionally, both dendritic cell (DC) and inflammatory macrophage (IM) cell populations were significantly higher in *M. pneumoniae*-infected WT mice than in mock-infected and NLRP3 KO mice (Fig. 7C and D). Our results indicate that NLRP3 is critical for recruitment and activation of neutrophils, DCs, and IMs during *M. pneumoniae* infection.

DISCUSSION

In this study, we characterized the role of NLRP3 in the innate immune response against *M. pneumoniae*. Infection of mouse BMDMs with *M. pneumoniae* stimulated inflammasome complex formation that resulted in activation of caspase-1 and secretion of IL-1β into cell culture supernatants. Inflammasome activation was found to be dependent on the proteins NLRP3, ASC, and procaspase-1. In addition, the MyD88/NF-κB signaling pathway was essential for increasing gene expression of pro-IL-1β and IL-6 following *M. pneumoniae* infection. We then utilized the C57BL/6 animal model in order to study the physiological relevance of NLRP3 during *M. pneumoniae* infection. Mice that were deficient in NLRP3 expression were unable to secrete IL-1β into the lungs during infection. However, with TLR-MyD88-NF-κB signaling unaffected, NLRP3 KO mice were still capable of detecting *M. pneumoniae*, resulting in secretion of IL-6 at levels comparable to those of WT mice. Lack of IL-1β-mediated inflammation in infected NLRP3 KO mice resulted in a significantly diminished ability to clear

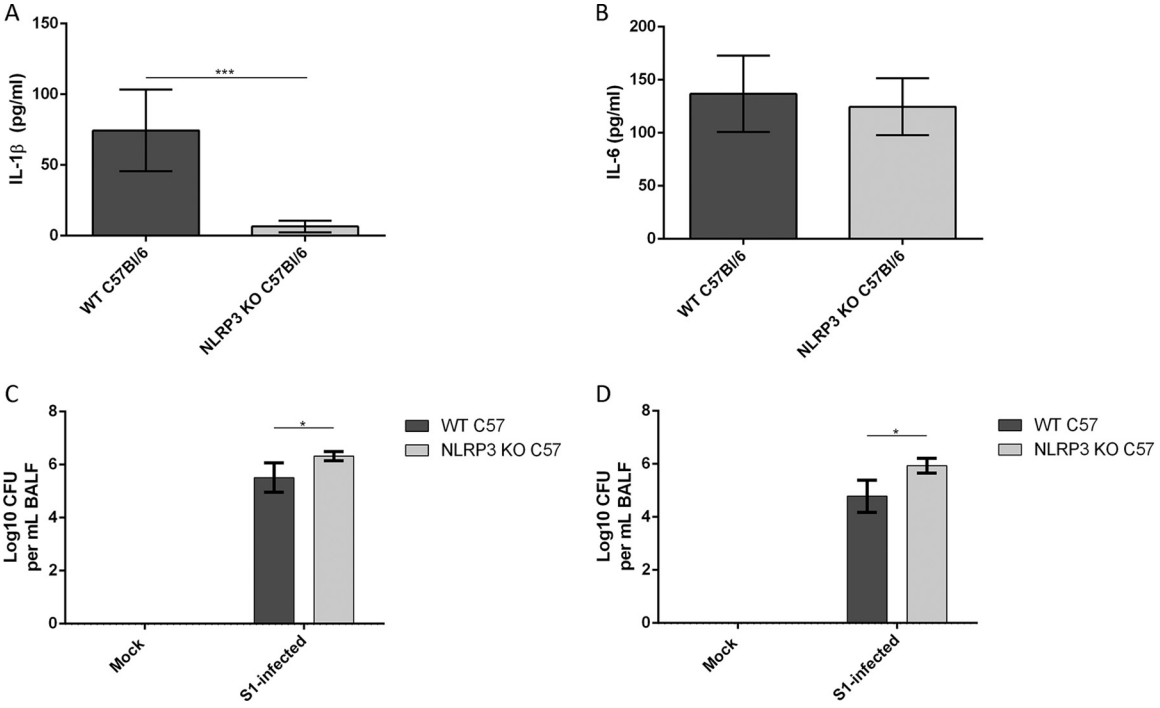

FIG 6 NLRP3 is required to elicit IL-1β production and to partly inhibit *M. pneumoniae* growth *in vivo*. WT and NLRP3 KO C57BL/6 mice were infected with *M. pneumoniae* (7 $\log_{10}$ CFU) for 2 days and 7 days. IL-1β (A) and IL-6 (B) levels in BALFs from 2-day-infected lungs were measured by ELISA. BALFs from mice at 2 days (C) and 7 days (D) postinfection were also analyzed for quantification of *M. pneumoniae* genomes by qPCR. *, $P < 0.05$; ***, $P < 0.001$.

M. pneumoniae from the lungs. We observed that loss of the IL-1β-mediated inflammatory response resulted in inadequate trafficking and activation of innate immune cells in the lungs, including neutrophils, dendritic cells (DCs), and inflammatory macrophages (IMs). These findings suggest an important role for NLRP3 in activating the inflammatory response for the host defense against *M. pneumoniae* infection.

M. pneumoniae-mediated disease progression is markedly influenced by mycoplasma virulence factors and the host proinflammatory response during acute infection (15, 23, 26, 27). The innate immune defense against invading respiratory pathogens must be carefully controlled in order to suppress pathogen growth and minimize collateral damage to the lungs caused by both virulence factors and hyperinflammation (28). In this study, we utilized type 2 strain *M. pneumoniae* S1 due to its physiological relevance as a human clinical isolate and potential to stimulate enhanced inflammation and pathology during infection (29). We previously reported that *M. pneumoniae* CARDS toxin selectively ADP-ribosylates NLRP3, a homeostatic sensor protein important for regulating the inflammatory response via assembly of the inflammasome complex, thereby activating the NLRP3 inflammasome (18). While detection of a pathogen triggers expression of proinflammatory cytokines, such as pro-IL-1β, it is the inflammasome complex that is critical for facilitating caspase-1 activation and processing of pro-IL-1β into biologically active IL-1β. Numerous studies have highlighted the importance of NLRP3 in determining the outcome of host-pathogen interactions (30–33). Although the pathological outcomes of *M. pneumoniae* infection have been well studied for decades, information on the mechanism of the inflammatory response to *M. pneumoniae* is limited.

Infection of macrophages with *M. pneumoniae* S1 resulted in a classical proinflammatory response, whereby IL-6 secretion occurred early and was closely followed by inflammasome activation and IL-1β secretion (Fig. 1). *M. pneumoniae* infection was confirmed by detection of P1 adhesin and CARDS toxin, two important virulence factors, in lysates of infected macrophages (Fig. 1E). In contrast, *M. pneumoniae*

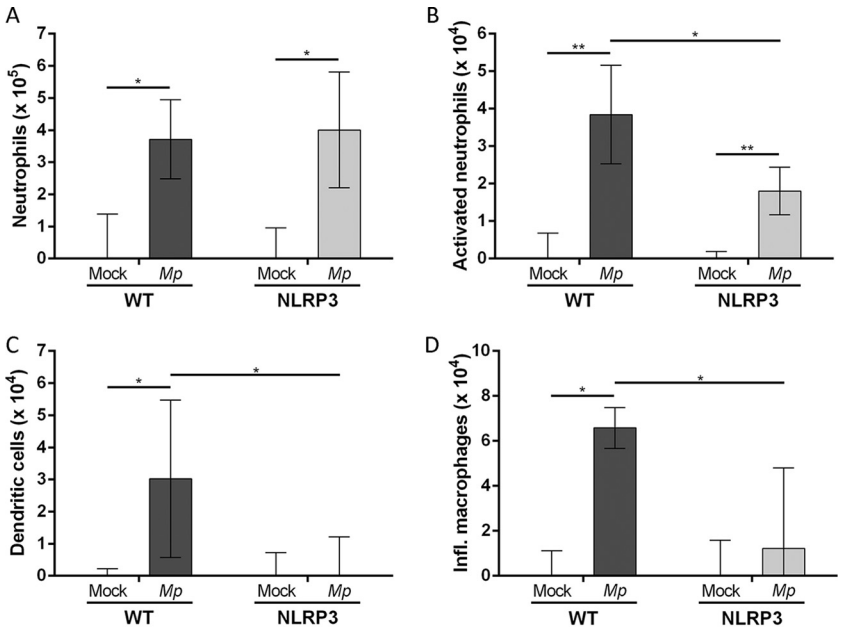

FIG 7 Characterization of innate immune cell populations in lungs of WT and NLRP3 KO C57BL/6 mice infected with *M. pneumoniae* S1 for 2 days. Lungs from mock-infected or S1-infected WT and NLRP3 KO C57BL/6 mice were harvested, digested, and analyzed by fluorescence-activated cell sorting. Identified cell populations include total neutrophils (A), activated neutrophils (B), dendritic cells (C), and inflammatory macrophages (D). Cell populations in infected lungs were normalized to mock-infected cell populations by subtracting values of the uninfected controls from those of the infected animals. *, $P < 0.05$; **, $P < 0.01$.

infection of NLRP3 KO macrophages resulted in drastically reduced IL-1β secretion compared to levels in infected WT macrophages (Fig. 2A), whereas IL-6 secretion was unaffected (Fig. 2B). The drastic reduction in IL-1β secretion was due to the inability to process the cytokine since pro-IL-1β protein levels in infected NLRP3 KO BMDMs were comparable to, if not slightly higher than, those in WT BMDMs. Lack of NLRP3 expression prevented inflammasome complex formation, leading to hindered caspase-1 activation and IL-β processing. Interestingly, although we detected low levels of IL-1β in supernatants of infected NLRP3 KO BMDMs by ELISA, we were unable to detect the IL-1β p17 protein by immunoblotting (Fig. 2A and C). It is possible that pro-IL-1β was being detected in the supernatant by ELISA, likely a result of low levels of macrophage cell death after 8 h of infection. An alternative mechanism may involve use of the protein AIM2, which activates the inflammasome in response to detecting double-stranded DNA (34). When analyzing protein levels of CARDS toxin and P1 adhesin, we detected no discernible differences between infected NLRP3 KO and WT BMDMs. Thus, NLRP3 likely does not directly affect *M. pneumoniae* growth or CARDS toxin expression. Indeed, through the course of our study, we observed no difference in patterns of CARDS toxin or P1 adhesin protein levels, and, as such, we included immunoblots of these proteins in only Fig. 1 and 2. In comparison to infection of NLRP3 KO macrophages, infection of NLRP1 KO macrophages with *M. pneumoniae* yielded secretion levels of both IL-1β and IL-6 comparable to those in infected WT macrophages. NLRP1 is a closely related inflammasome sensor to NLRP3 but is activated in response to different stimuli, such as anthrax lethal toxin, muramyl dipeptide (MDP), and *Toxoplasma gondii* (35). This further reinforces the specific requirement of the NLRP3 inflammasome for IL-1β production during *M. pneumoniae* infection.

Given the important roles of ASC and caspase-1 during inflammasome function, we next tested the requirements of these proteins for inflammasome-dependent IL-1β secretion. We observed complete loss of IL-1β secretion, but not pro-IL-1β expression, in infected ASC KO and caspase-1 KO BMDMs (Fig. 3A, C, and D). Infected ASC KO and

caspase-1 KO BMDMs were still able to secrete levels of IL-6 equivalent to those of infected WT BMDMs (Fig. 3B). Thus, all three inflammasome components (NLRP3, ASC, and caspase-1) are required during *M. pneumoniae* infection for IL-1β processing but are not necessary for pro-IL-1β protein expression or IL-6 secretion. These data also indicate that the cellular machinery required for detection of *M. pneumoniae* during infection remained intact, allowing the BMDMs to express and secrete IL-6 into the supernatant. Our results demonstrate that *M. pneumoniae* infection in macrophages triggers the NLRP3/ASC/caspase-1 inflammasome, leading to activation and secretion of IL-1β. These data support other published reports of the NLRP3/ASC/caspase-1 inflammasome as a key mediator of inflammation during bacterial infection (33, 36).

Membrane-bound pattern recognition receptors (PRRs), such as Toll-like receptors (TLRs), are important for detecting pathogen-associated molecular patterns (PAMPs) during infection (25). *M. pneumoniae* is an atypical bacterium that does not possess a cell wall and, as such, does not contain classical TLR triggers, like lipopolysaccharide (LPS). A limited number of studies have identified *M. pneumoniae* surface lipoproteins that are capable of triggering TLR-MyD88 activation, leading to production of proinflammatory cytokines such as IL-6 (37, 38). Stimulation of IL-6 in the KO BMDMs is likely due to sensing of *M. pneumoniae* lipoproteins by TLRs. MyD88 is critical for executing a signal transduction cascade that activates the transcription factor NF-κB, which translocates to the nucleus to express proinflammatory genes. TLR/MyD88/NF-κB activation serves as a first signal to the target cell, indicating that a pathogen is present and that upregulation of proinflammatory genes is necessary to successfully combat the pathogen (39). A second signal, such as extracellular ATP, reactive oxygen species (ROS), or potassium efflux, is required to trigger assembly of the inflammasome complex, leading to caspase-1 activation and IL-1β processing (18). The importance of the MyD88/NF-κB pathway for detection and clearance of *M. pneumoniae* by macrophages in the lungs of C57BL/6 mice has been previously explored (40). Here, we identified the MyD88/NF-κB pathway as being essential for IL-1β secretion in response to *M. pneumoniae* infection (Fig. 4 and 5). Pharmacological inhibition of NF-κB by BAY11-7082 (Fig. 4) or the absence of MyD88 (Fig. 5) resulted in abolishment of IL-1β and IL-6 secretion and expression, further demonstrating the importance of the MyD88/NF-κB pathway in initiating the proinflammatory response during *M. pneumoniae* infection. Importantly, caspase-1 activation was still readily detected in BAY11-7082-treated BMDMs (Fig. 4C) or MyD88 KO BMDMs (Fig. 5C) infected with *M. pneumoniae*, indicating that the macrophage's ability to activate inflammasome remained intact. It was the inhibition of proinflammatory gene upregulation (via inhibition of MyD88/NF-κB) that led to the abolishment of IL-1β and IL-6 secretion. DMSO-treated macrophages infected with *M. pneumoniae* displayed slightly dampened pro-IL-1β protein levels at 16 h postinfection, possibly due to mild toxic effects of DMSO at low ($<$0.1%) concentrations. These data reinforce previous findings (40) on the importance of the macrophage MyD88/NF-κB signaling pathway in initiating the proinflammatory response during *M. pneumoniae* infection.

Next, we tested the physiological role of NLRP3 during *M. pneumoniae* infection in the C57BL/6 animal model. In agreement with our *in vitro* findings, NLRP3 KO mice infected with *M. pneumoniae*, in contrast to WT mice, failed to secrete IL-1β into the airway (Fig. 6A); IL-6 secretion was unaffected (Fig. 6B). No detectable levels of IL-1β or IL-6 were measurable in the BALFs of infected mice at 7 days postinfection. Interestingly, bacterial clearance was compromised in NLRP3 KO mice compared with clearance in WT mice at both 2 days and 7 days postinfection (Fig. 6C and D, respectively). At 2 days postinfection, NLRP3 KO mice had a 5-fold-higher bacterial burden than WT mice. This phenomenon was more pronounced at 7 days postinfection, with NLRP3 mice displaying a 10-fold-higher bacterial burden than WT mice. It is important to note that qPCR analysis revealed a significant difference in *M. pneumoniae* genome equivalents between infected WT and NLRP3 KO mice; however, the data do not signify viable mycoplasma CFU counts. Strikingly similar NLRP3-associated bacterial clearance phenomena have been observed with *Streptococcus pneumoniae* and *Helicobacter pylori*

(41, 42). Thus, our data support the notion that NLRP3 is critical for triggering the IL-1β-mediated inflammatory response early during acute infection. Lack of this response diminishes *M. pneumoniae* clearance from the airways.

It is well established that clearance of *M. pneumoniae* is facilitated by phagocytic cells of the innate immune system that are either recruited to or resident in the lungs during infection. Therefore, we explored the role of NLRP3 in recruitment and activation of neutrophils, DCs, and IMs into the lungs during *M. pneumoniae* infection. Neutrophils, DCs, and IMs play a critical role in bacterial clearance. Through flow cytometry analysis, we observed that trafficking of CD11b$^+$ F4/80$^-$ neutrophils into the lungs of *M. pneumoniae*-infected mice is significantly increased at 2 days postinfection compared to levels in mock-infected controls. However, there were no significant differences in total neutrophils between infected NLRP3 KO and WT mice (Fig. 7A). Upon detailed analysis, we observed significantly reduced numbers of Ly6G$^+$ activated neutrophils in infected NLRP3 KO mice compared to numbers in WT mice (Fig. 7B). Furthermore, we noted a much more drastic absence of CD11c$^+$ F4/80$^-$ DCs (Fig. 7C) and CD11c$^-$ F4/80$^+$ CD11b$^+$ IMs (Fig. 7D) in infected NLRP3 KO mice than in WT mice. These results highlight an important role of IL-1β in recruiting and activating in the lung innate immune cells that are critical for bacterial clearance. Our results are in line with inflammasome regulation of the innate immune response during infection by altering (i) the function of DCs and macrophages (43), (ii) the inflammatory response and adaptive immune response (44), and (iii) cell death pathways (i.e., apoptosis and pyroptosis).

The current study provides insight into the host-pathogen interaction during acute *M. pneumoniae* infection. The initial stages of *M. pneumoniae* infection are characterized by mycoplasma adherence to the host respiratory epithelium and production of mycoplasma virulence factors, especially large amounts of the ADP-ribosylating and vacuolating CARDS toxin (8, 12). Cytadherence and subsequent colonization of *M. pneumoniae* and synthesis of CARDS toxin trigger a strong proinflammatory response in the host, leading to production of proinflammatory cytokines (IL-1β, IL-6, and TNF-α), peribronchiolar infiltration of immune cells, and pulmonary injury (15, 45). Our results detail the specific requirement of the NLRP3 inflammasome in IL-1β secretion and in regulating the inflammatory response during *M. pneumoniae* infection. Also, we demonstrate that the IL-1β-mediated response is essential for activation of innate immune cells involved in clearance of *M. pneumoniae* during infection. These data reinforce the relevance of examining the mechanism of action of *M. pneumoniae* CARDS toxin on the host inflammatory response during *M. pneumoniae* acute infection. We envision that CARDS toxin is the most significant virulence factor produced by *M. pneumoniae* during infection and that CARDS toxin-mediated activation of the NLRP3 inflammasome benefits *M. pneumoniae* colonization and/or survival through a yet uncharacterized mechanism(s). It is possible that CARDS toxin-mediated alteration of normal NLRP3 function results in a hyperinflammatory state that hinders *M. pneumoniae* clearance during later stages of infection. A recent study found that temporally altered NLRP3 activation resulted in a detrimental inflammatory response that failed to protect the host from influenza A virus (IAV) infection (46). Although our data suggest that NLRP3 is protective during *M. pneumoniae* infection under the conditions we analyzed, it is unknown whether persistent bacterial infection and CARDS toxin synthesis trigger a greater than normal or prolonged inflammatory state. We expect that, depending on the infectious dose, toxin expression level, and state of infection, CARDS toxin-activated NLRP3 can either protect the host or alter the host's ability to control the inflammatory response, allowing *M. pneumoniae* to take advantage of an exhausted immune state. In order to address these questions, our future studies will utilize a CARDS toxin-deficient mutant of *M. pneumoniae*. These studies will help us decipher the mechanism(s) by which CARDS toxin impacts the immune response at the cellular level to provide an advantage for *M. pneumoniae* during infection. We will also focus our studies on the function of host innate immune cells affected by CARDS toxin during the course of *M. pneumoniae* infection. Understanding the downstream consequences of NLRP3 inflam-

masome activation by CARDS toxin will offer insights into new therapeutic approaches that control and prevent mycoplasma infection and inflammatory disease progression.

MATERIALS AND METHODS

Organism and growth conditions. *M. pneumoniae* type 2 strain S1 was grown in SP4 broth in T-150 cell culture flasks at 37°C for 3 days. Adherent mycoplasma colonies were gently washed once with warm SP4 broth and harvested in 5 ml of SP4 broth by scraping. Cultures were then passed through a 25-gauge needle three times in a 50-ml conical tube. Utilizing this method, we consistently achieved a final concentration of 5×10^9 CFU per ml. Viable mycoplasma were determined by assaying color change units (CCU) and CFU in SP4 broth and agar plates.

Cell culture. Bone marrow-derived macrophages (BMDMs) were obtained by harvesting bone marrow from femurs and tibias of 8- to 12-week-old C57BL/6 mice as described previously (47). Briefly, bone marrow cells were differentiated into macrophages by culturing in 10-cm petri dishes for 10 days in RPMI 1640 medium containing 10% fetal bovine serum (FBS), 100 IU/ml penicillin, 100 μg/ml streptomycin, and 20 ng/ml recombinant granulocyte-macrophage colony-stimulating factor (GM-CSF; Peprotech). Macrophages were washed three times with ice-cold Dulbecco's phosphate-buffered saline (DPBS) and incubated for 30 min at 4°C with DPBS supplemented with 5 mM EDTA. Cells were removed through gentle pipetting, centrifuged, resuspended in complete BMDM medium, and transferred to 12-well cell culture plates at a concentration of 5×10^5 cells per well, in a final volume of 1 ml of complete medium. Cells were allowed to recover for 48 h before any treatments or infections were performed. BMDMs were infected with *M. pneumoniae* (5×10^7 CFU in 10 μl of SP4 broth) to achieve a final multiplicity of infection (MOI) of 100 mycoplasmas per BMDM in a total of 1 ml of complete medium; this MOI was determined to be optimal for assessing BMDM responsiveness. Supernatants and cells were harvested at various times postinfection for ELISA and immunoblot analysis. Wild-type (WT) and NLRP3 KO C57BL/6 mice were purchased from Jackson Laboratories. MyD88 KO mice were provided by Michael Berton (University of Texas Health Science Center, San Antonio [UTHSCSA], TX). ASC KO and caspase-1 KO BMDMs were provided by Norberto González-Juarbe and Carlos J. Orihuela (University of Alabama at Birmingham).

Animals. Eight- to 12-week-old male and female WT and NLRP3 KO C57BL/6 mice were anesthetized via isoflurane in a rodent anesthesia machine as described previously (15). Following stable sedation, mice were infected intranasally (i.n.) once with 7 $\log_{10}$ CFU of *M. pneumoniae* in 40 μl of SP4 broth. Uninfected WT and NLRP3 KO mice received a single 40-μl dose of sterile SP4 broth i.n.; animals from each group were euthanized, and samples were collected at 2 days and 7 days postinfection for functional studies. Then, cytokine/chemokine, flow cytometry, and mycoplasma genome analyses were performed. Mice were housed in filter-top cages in a biosafety level 2 (BSL2) vivarium, and animal guidelines were strictly followed in accordance with the Institutional Animal Care and Use Committee at the University of Texas Health Science Center at San Antonio.

Sample collection and analysis. Mouse serum and bronchoalveolar lavage fluids (BALFs) were collected at 2 and 7 days postinfection ($n = 4$ per group). BALF was harvested using 1.5 ml of phosphate-buffered saline (PBS) with complete protease inhibitor cocktail (Roche). For *M. pneumoniae* genome quantification, DNA was purified from 200 μl of unclarified BALF and analyzed for CARDS toxin gene copy numbers using a StepOnePlus system (Applied Biosystems) as described previously (29, 48). The remaining BALF was clarified by centrifugation, aliquoted, and frozen at −80°C until further analysis.

Multiplex cytokine bead assay and ELISA kits. A 25-plex proinflammatory cytokine/chemokine panel assay kit was purchased from Millipore, and multiplex analysis was performed at the Bioanalytics and Single-Cell Core (BASiC) at UTHSCSA. ELISA kits specific for mouse IL-1β and mouse IL-6 were purchased from Affymetrix-eBioscience.

Reagents and antibodies. BAY11-7082, an inhibitor that prevents activation of NF-κB (49), was purchased from Sigma and reconstituted in cell culture-grade DMSO (Sigma). For immunoblotting, primary antibodies (dilutions) were purchased as follows: goat anti-mouse IL-1β p17 (1:2,000) from R&D Systems, mouse anti-actin (1:20,000) from Sigma, rabbit anti-mouse caspase-1 p10 (1:500) from Santa Cruz, and mouse anti-ASC (1:1,000) from EMD Millipore. Rabbit anti-CARDS toxin (1:20,000) and rabbit anti-P1 adhesin (1:20,000) were produced in-house. The following horseradish peroxidase (HRP)-conjugated secondary antibodies (dilutions) were purchased from Jackson ImmunoResearch: donkey anti-goat (1:2,500), goat anti-mouse (1:5,000), and goat anti-rabbit (1:5,000).

Flow cytometry analysis. Lungs from *M. pneumoniae* strain S1-infected mice at 2 days postinfection were harvested, gently chopped, and digested with collagenase (1 mg/ml; Sigma) in RPMI medium with gentle agitation for 30 min. The digested tissue was then passed through 70-μm- and 40-μm-pore-size cell strainers (Falcon) and treated with ammonium-chloride-potassium (ACK) lysing buffer for 3 min to lyse erythrocytes. Cells were then washed, resuspended in ice-cold staining buffer (1% bovine serum albumin, 10 mM EDTA, 0.1% sodium azide in 1× Gibco DPBS), and counted. For staining, 0.5 μg of each of the following antibodies was used per sample of 10^6 cells: rat anti-mouse CD16/CD32 Fc Block, phycoerythrin (PE)-conjugated anti-mouse CD45, and PE-Cy7 anti-mouse CD11b (BD Biosciences); Alexa Fluor 647 anti-mouse F4/80, Pacific Blue anti-mouse CD11c, and peridinin chlorophyll protein (PerCP)-Cy5.5 anti-mouse Ly-6G (Biolegend). UltraComp eBeads (eBioscience) and ghost dyes (Tonbo) were used for single-color compensation controls and exclusion of dead cells, respectively. Samples were fixed with 2% paraformaldehyde in staining buffer prior to analysis.

Statistical analysis. Data were checked for normal distribution and then analyzed using GraphPad Prism, version 6.0, and Microsoft Excel software. Where shown, data correspond to means ± standard deviations (SD). Data in Fig. 7A and B were analyzed using Student's *t* test on Microsoft excel. All other

data were analyzed using two-way analysis of variance (ANOVA) with Bonferroni's multiple-comparison test in GraphPad Prism. Data were considered significant different at a P value of <0.05.

SUPPLEMENTAL MATERIAL

Supplemental material for this article may be found at https://doi.org/10.1128/IAI.00548-17.

SUPPLEMENTAL FILE 1, PDF file, 0.1 MB.

ACKNOWLEDGMENTS

J.A.S. is supported by NIH grant K12GM111726. T.-H.C., S.B., and T.R.K. are supported by NIH grant R21AI118051. S.B. is supported by AI083387. J.B.B. and coauthors are supported by NIH grant U19AI070412. We thank the Bioanalytics and Single-Cell Core (BASiC) at UTHSCSA for the data generated using the Luminex Flexmap platform. The BASiC is supported by the Cancer Prevention Institute of Texas (RP150600) and the Office of Vice President of Research, UTHSCSA. Flow cytometry data were generated in the Flow Cytometry Shared Facility, which is supported by UTHSCSA, NIH-NCI P30 CA054174-20 (Cancer Therapy and Research Center [CTRC] at UTHSCSA), and UL1 TR001120 (CTSA grant).

REFERENCES

1. Guilbert TW, Denlinger LC. 2010. Role of infection in the development and exacerbation of asthma. Expert Rev Respir Med 4:71–83. https://doi.org/10.1586/ers.09.60.
2. Jain S, Williams DJ, Arnold SR, Ampofo K, Bramley AM, Reed C, Stockmann C, Anderson EJ, Grijalva CG, Self WH, Zhu Y, Patel A, Hymas W, Chappell JD, Kaufman RA, Kan JH, Dansie D, Lenny N, Hillyard DR, Haynes LM, Levine M, Lindstrom S, Winchell JM, Katz JM, Erdman D, Schneider E, Hicks LA, Wunderink RG, Edwards KM, Pavia AT, McCullers JA, Finelli L, Team CES. 2015. Community-acquired pneumonia requiring hospitalization among U.S. children. N Engl J Med 372:835–845. https://doi.org/10.1056/NEJMoa1405870.
3. Jain S, Self WH, Wunderink RG, Fakhran S, Balk R, Bramley AM, Reed C, Grijalva CG, Anderson EJ, Courtney DM, Chappell JD, Qi C, Hart EM, Carroll F, Trabue C, Donnelly HK, Williams DJ, Zhu Y, Arnold SR, Ampofo K, Waterer GW, Levine M, Lindstrom S, Winchell JM, Katz JM, Erdman D, Schneider E, Hicks LA, McCullers JA, Pavia AT, Edwards KM, Finelli L, CDC EPIC Study Team. 2015. Community-acquired pneumonia requiring hospitalization among U.S. adults. N Engl J Med 373:415–427. https://doi.org/10.1056/NEJMoa1500245.
4. Waites KB, Talkington DF. 2004. *Mycoplasma pneumoniae* and its role as a human pathogen. Clin Microbiol Rev 17:697–728. https://doi.org/10.1128/CMR.17.4.697-728.2004.
5. Yamada M, Buller R, Bledsoe S, Storch GA. 2012. Rising rates of macrolide-resistant *Mycoplasma pneumoniae* in the central United States. Pediatr Infect Dis J 31:409–400. https://doi.org/10.1097/INF.0b013e318247f3e0.
6. Wang Y, Qiu S, Yang G, Song L, Su W, Xu Y, Jia L, Wang L, Hao R, Zhang C, Liu J, Fu X, He J, Zhang J, Li Z, Song H. 2012. An outbreak of *Mycoplasma pneumoniae* caused by a macrolide-resistant isolate in a nursery school in China. Antimicrob Agents Chemother 56:3748–3752. https://doi.org/10.1128/AAC.00142-12.
7. Baseman JB, Cole RM, Krause DC, Leith DK. 1982. Molecular basis for cytadsorption of *Mycoplasma pneumoniae*. J Bacteriol 151:1514–1522.
8. Tryon W, Baseman JB. 1992. Pathogenic determinants and mechanisms, p 457–471. *In* Maniloff J, McElhaney RN, Finch LR, Baseman JB (ed), Mycoplasmas: molecular biology and pathogenesis. American Society for Microbiology, Washington, DC.
9. Cartner SC, Lindsey JR, Gibbs-Erwin J, Cassell GH, Simecka JW. 1998. Roles of innate and adaptive immunity in respiratory mycoplasmosis. Infect Immun 66:3485–3491.
10. Baseman JB, Tully JG. 1997. Mycoplasmas: sophisticated, reemerging, and burdened by their notoriety. Emerg Infect Dis 3:21–32. https://doi.org/10.3201/eid0301.970103.
11. Kannan TR, Provenzano D, Wright JR, Baseman JB. 2005. Identification and characterization of human surfactant protein A binding protein of *Mycoplasma pneumoniae*. Infect Immun 73:2828–2834. https://doi.org/10.1128/IAI.73.5.2828-2834.2005.
12. Kannan TR, Baseman JB. 2006. ADP-ribosylating and vacuolating cytotoxin of *Mycoplasma pneumoniae* represents unique virulence determinant among bacterial pathogens. Proc Natl Acad Sci U S A 103:6724–6729. https://doi.org/10.1073/pnas.0510644103.
13. Kannan TR, Krishnan M, Kumaraguruparan R, Becker A, Pakhomova ON, Hart PJ, Baseman JB. 2014. Functional mapping of community acquired respiratory distress syndrome (CARDS) toxin of *Mycoplasma pneumoniae* defines regions with ADP-ribosyltransferase, vacuolating, and receptor-binding activities. Mol Microbiol 93:568–581. https://doi.org/10.1111/mmi.12680.
14. Becker A, Kannan TR, Taylor AB, Pakhomova ON, Zhang Y, Somarajan SR, Galaleldeen A, Holloway SP, Baseman JB, Hart PJ. 2015. Structure of CARDS toxin, a unique ADP-ribosylating and vacuolating cytotoxin from *Mycoplasma pneumoniae*. Proc Natl Acad Sci U S A 112:5165–5170. https://doi.org/10.1073/pnas.1420308112.
15. Hardy RD, Coalson JJ, Peters J, Chaparro A, Techasaensiri C, Cantwell AM, Kannan TR, Baseman JB, Dube PH. 2009. Analysis of pulmonary inflammation and function in the mouse and baboon after exposure to *Mycoplasma pneumoniae* CARDS toxin. PLoS One 4:e7562. https://doi.org/10.1371/journal.pone.0007562.
16. Kannan TR, Musatovova O, Balasubramanian S, Cagle M, Jordan JL, Krunkosky TM, Davis A, Hardy RD, Baseman JB. 2010. *Mycoplasma pneumoniae* community acquired respiratory distress syndrome toxin expression reveals growth phase and infection-dependent regulation. Mol Microbiol 76:1127–1141. https://doi.org/10.1111/j.1365-2958.2010.07092.x.
17. Peters J, Singh H, Brooks EG, Diaz J, Kannan TR, Coalson JJ, Baseman JG, Cagle M, Baseman JB. 2011. Persistence of community-acquired respiratory distress syndrome toxin-producing *Mycoplasma pneumoniae* in refractory asthma. Chest 140:401–407. https://doi.org/10.1378/chest.11-0221.
18. Bose S, Segovia JA, Somarajan SR, Chang TH, Kannan TR, Baseman JB. 2014. ADP-ribosylation of NLRP3 by *Mycoplasma pneumoniae* CARDS toxin regulates inflammasome activity. mBio 5:e02186-14. https://doi.org/10.1128/mBio.02186-14.
19. Broz P, von Moltke J, Jones JW, Vance RE, Monack DM. 2010. Differential requirement for caspase-1 autoproteolysis in pathogen-induced cell death and cytokine processing. Cell Host Microbe 8:471–483. https://doi.org/10.1016/j.chom.2010.11.007.
20. Netea MG, Nold-Petry CA, Nold MF, Joosten LA, Opitz B, van der Meer JH, van de Veerdonk FL, Ferwerda G, Heinhuis B, Devesa I, Funk CJ, Mason RJ, Kullberg BJ, Rubartelli A, van der Meer JW, Dinarello CA. 2009. Differential requirement for the activation of the inflammasome for processing and release of IL-1β in monocytes and macrophages. Blood 113:2324–2335. https://doi.org/10.1182/blood-2008-03-146720.
21. Medzhitov R, Preston-Hurlburt P, Kopp E, Stadlen A, Chen C, Ghosh S, Janeway CA, Jr. 1998. MyD88 is an adaptor protein in the hToll/IL-1 receptor family signaling pathways. Mol Cell 2:253–258. https://doi.org/10.1016/S1097-2765(00)80136-7.

22. Athamna A, Kramer MR, Kahane I. 1996. Adherence of *Mycoplasma pneumoniae* to human alveolar macrophages. FEMS Immunol Med Microbiol 15:135–141. https://doi.org/10.1111/j.1574-695X.1996.tb00064.x.
23. Fonseca-Aten M, Rios AM, Mejias A, Chavez-Bueno S, Katz K, Gomez AM, McCracken GH, Jr, Hardy RD. 2005. *Mycoplasma pneumoniae* induces host-dependent pulmonary inflammation and airway obstruction in mice. Am J Respir Cell Mol Biol 32:201–210. https://doi.org/10.1165/rcmb.2004-0197OC.
24. Kazachkov MY, Hu PC, Carson JL, Murphy PC, Henderson FW, Noah TL. 2002. Release of cytokines by human nasal epithelial cells and peripheral blood mononuclear cells infected with *Mycoplasma pneumoniae*. Exp Biol Med (Maywood) 227:330–335. https://doi.org/10.1177/153537020222700505.
25. Kawai T, Akira S. 2006. TLR signaling. Cell Death Differ 13:816–825. https://doi.org/10.1038/sj.cdd.4401850.
26. Shimizu T, Kida Y, Kuwano K. 2011. Cytoadherence-dependent induction of inflammatory responses by *Mycoplasma pneumoniae*. Immunology 133:51–61. https://doi.org/10.1111/j.1365-2567.2011.03408.x.
27. Shimizu T, Kida Y, Kuwano K. 2008. *Mycoplasma pneumoniae*-derived lipopeptides induce acute inflammatory responses in the lungs of mice. Infect Immun 76:270–277. https://doi.org/10.1128/IAI.00955-07.
28. Han W, Joo M, Everhart MB, Christman JW, Yull FE, Blackwell TS. 2009. Myeloid cells control termination of lung inflammation through the NF-κB pathway. Am J Physiol Lung Cell Mol Physiol 296:L320–L327. https://doi.org/10.1152/ajplung.90485.2008.
29. Techasaensiri C, Tagliabue C, Cagle M, Iranpour P, Katz K, Kannan TR, Coalson JJ, Baseman JB, Hardy RD. 2010. Variation in colonization, ADP-ribosylating and vacuolating cytotoxin, and pulmonary disease severity among *Mycoplasma pneumoniae* strains. Am J Respir Crit Care Med 182:797–804. https://doi.org/10.1164/rccm.201001-0080OC.
30. Abdul-Sater AA, Said-Sadier N, Padilla EV, Ojcius DM. 2010. Chlamydial infection of monocytes stimulates IL-1β secretion through activation of the NLRP3 inflammasome. Microbes Infect 12:652–661. https://doi.org/10.1016/j.micinf.2010.04.008.
31. Kim S, Bauernfeind F, Ablasser A, Hartmann G, Fitzgerald KA, Latz E, Hornung V. 2010. *Listeria monocytogenes* is sensed by the NLRP3 and AIM2 inflammasome. Eur J Immunol 40:1545–1551. https://doi.org/10.1002/eji.201040425.
32. Arlehamn CS, Evans TJ. 2011. *Pseudomonas aeruginosa* pilin activates the inflammasome. Cell Microbiol 13:388–401. https://doi.org/10.1111/j.1462-5822.2010.01541.x.
33. Kim JJ, Jo EK. 2013. NLRP3 inflammasome and host protection against bacterial infection. J Korean Med Sci 28:1415–1423. https://doi.org/10.3346/jkms.2013.28.10.1415.
34. Rathinam VA, Jiang Z, Waggoner SN, Sharma S, Cole LE, Waggoner L, Vanaja SK, Monks BG, Ganesan S, Latz E, Hornung V, Vogel SN, Szomolanyi-Tsuda E, Fitzgerald KA. 2010. The AIM2 inflammasome is essential for host defense against cytosolic bacteria and DNA viruses. Nat Immunol 11:395–402. https://doi.org/10.1038/ni.1864.
35. Chavarria-Smith J, Vance RE. 2015. The NLRP1 inflammasomes. Immunol Rev 265:22–34. https://doi.org/10.1111/imr.12283.
36. Koizumi Y, Toma C, Higa N, Nohara T, Nakasone N, Suzuki T. 2012. Inflammasome activation via intracellular NLRs triggered by bacterial infection. Cell Microbiol 14:149–154. https://doi.org/10.1111/j.1462-5822.2011.01707.x.
37. Shimizu T, Kida Y, Kuwano K. 2007. Triacylated lipoproteins derived from *Mycoplasma pneumoniae* activate nuclear factor-κB through Toll-like receptors 1 and 2. Immunology 121:473–483. https://doi.org/10.1111/j.1365-2567.2007.02594.x.
38. Shimizu T, Kimura Y, Kida Y, Kuwano K, Tachibana M, Hashino M, Watarai M. 2014. Cytadherence of *Mycoplasma pneumoniae* induces inflammatory responses through autophagy and Toll-like receptor 4. Infect Immun 82:3076–3086. https://doi.org/10.1128/IAI.01961-14.
39. Bauernfeind FG, Horvath G, Stutz A, Alnemri ES, MacDonald K, Speert D, Fernandes-Alnemri T, Wu J, Monks BG, Fitzgerald KA, Hornung V, Latz E. 2009. Cutting edge: NF-κB activating pattern recognition and cytokine receptors license NLRP3 inflammasome activation by regulating NLRP3 expression. J Immunol 183:787–791. https://doi.org/10.4049/jimmunol.0901363.
40. Lai JF, Zindl CL, Duffy LB, Atkinson TP, Jung YW, van Rooijen N, Waites KB, Krause DC, Chaplin DD. 2010. Critical role of macrophages and their activation via MyD88-NFκB signaling in lung innate immunity to *Mycoplasma pneumoniae*. PLoS One 5:e14417. https://doi.org/10.1371/journal.pone.0014417.
41. Semper RP, Mejias-Luque R, Gross C, Anderl F, Muller A, Vieth M, Busch DH, Prazeres da Costa C, Ruland J, Gross O, Gerhard M. 2014. *Helicobacter pylori*-induced IL-1β secretion in innate immune cells is regulated by the NLRP3 inflammasome and requires the cag pathogenicity island. J Immunol 193:3566–3576. https://doi.org/10.4049/jimmunol.1400362.
42. Witzenrath M, Pache F, Lorenz D, Koppe U, Gutbier B, Tabeling C, Reppe K, Meixenberger K, Dorhoi A, Ma J, Holmes A, Trendelenburg G, Heimesaat MM, Bereswill S, van der Linden M, Tschopp J, Mitchell TJ, Suttorp N, Opitz B. 2011. The NLRP3 inflammasome is differentially activated by pneumolysin variants and contributes to host defense in pneumococcal pneumonia. J Immunol 187:434–440. https://doi.org/10.4049/jimmunol.1003143.
43. Franchi L, Munoz-Planillo R, Nunez G. 2012. Sensing and reacting to microbes through the inflammasomes. Nat Immunol 13:325–332. https://doi.org/10.1038/ni.2231.
44. Vince JE, Silke J. 2016. The intersection of cell death and inflammasome activation. Cell Mol Life Sci 73:2349–2367. https://doi.org/10.1007/s00018-016-2205-2.
45. Hardy RD, Jafri HS, Olsen K, Hatfield J, Iglehart J, Rogers BB, Patel P, Cassell G, McCracken GH, Ramilo O. 2002. *Mycoplasma pneumoniae* induces chronic respiratory infection, airway hyperreactivity, and pulmonary inflammation: a murine model of infection-associated chronic reactive airway disease. Infect Immun 70:649–654. https://doi.org/10.1128/IAI.70.2.649-654.2002.
46. Tate MD, Ong JD, Dowling JK, McAuley JL, Robertson AB, Latz E, Drummond GR, Cooper MA, Hertzog PJ, Mansell A. 2016. Reassessing the role of the NLRP3 inflammasome during pathogenic influenza A virus infection via temporal inhibition. Sci Rep 6:27912. https://doi.org/10.1038/srep27912.
47. Segovia J, Sabbah A, Mgbemena V, Tsai SY, Chang TH, Berton MT, Morris IR, Allen IC, Ting JP, Bose S. 2012. TLR2/MyD88/NF-κB pathway, reactive oxygen species, potassium efflux activates NLRP3/ASC inflammasome during respiratory syncytial virus infection. PLoS One 7:e29695. https://doi.org/10.1371/journal.pone.0029695.
48. Winchell JM, Thurman KA, Mitchell SL, Thacker WL, Fields BS. 2008. Evaluation of three real-time PCR assays for detection of *Mycoplasma pneumoniae* in an outbreak investigation. J Clin Microbiol 46:3116–3118. https://doi.org/10.1128/JCM.00440-08.
49. Pierce JW, Schoenleber R, Jesmok G, Best J, Moore SA, Collins T, Gerritsen ME. 1997. Novel inhibitors of cytokine-induced IκBα phosphorylation and endothelial cell adhesion molecule expression show anti-inflammatory effects in vivo. J Biol Chem 272:21096–21103. https://doi.org/10.1074/jbc.272.34.21096.